Engineering Failure Analysis 163 (2024) 108571

Contents lists available at ScienceDirect

Engineering Failure Analysis

journal homepage: www.elsevier.com/locate/engfailanal

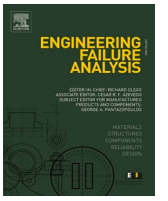

Review

Systematic review of experimental testing of masonry walls' failure: Comparative analysis and future directions

Jamiu A. Dauda [a,*], Ornella Iuorio [b], Imrose B. Muhit [c], Luis C.M. da Silva [b]

[a] School of Built Environment, Engineering and Computing, Leeds Beckett University, Leeds LS1 3HE, United Kingdom
[b] Department A.B.C., Politecnico di Milano, Piazza Leonardo da Vinci, 20133 Milan, Italy
[c] School of Computing, Engineering and Digital Technologies, Teesside University, Middlesbrough TS1 3BX, United Kingdom

ARTICLE INFO

Keywords:
Masonry wall
In-plane failure
Out-of-plane failure
Experimental testing
Failure patterns
Systematic review

ABSTRACT

The assessment of unreinforced masonry (URM) walls often involves experimental characterisation of their in-plane (IP) and out-of-plane (OOP) failure. While IP and OOP testing of URM walls is common, standardised testing methods are lacking, resulting in varied approaches. This study thus presents a systematic review of 54 selected articles to examine different masonry testing procedures through an analysis of specimen characterisation, testing arrangements, loading rate and failure patterns across various studies. The review highlights disparities in experimental approaches and stresses the need for uniform testing procedures or standardisation protocol to ensure consistency and reliability. Significantly, the review identifies a tendency to overlook real-world scenarios in testing, emphasising the importance of addressing this gap for comprehensive assessment of masonry walls. The study recommends further experimental studies on the effect of openings on walls, and the interaction between masonry walls and the slabs/connections with other walls/ring beams to enrich masonry behaviour understanding through both experimental and numerical approaches.

1. Introduction

Structural masonry construction has been widely used throughout history. The wider coverage of masonry construction in many parts of the world is often attributed to its low cost due to its relative ease of construction and the use of readily available local materials [1]. These materials can be clay brick units, concrete blocks, or building stones such as granite, limestone, or marble [1–3]. Brick units and concrete blocks are the most used materials for masonry construction and can be classified as unreinforced, reinforced, confined, and prestressed [2]. From the latter, unreinforced masonry (URM) structures are the most common since they rely on the arrangement of units that can be bonded together with mortar joints [1,4].

In URM structures, the load-bearing walls are the primary structural elements that may resist permanent, variable and accidental actions [5]. Depending on the actions, such elements can be governed by in-plane (IP) and out-of-plane (OOP) deformations [6], or by a combination of both. Generally, the failure of URM walls can lead to the partial or global collapse of the walls in OOP due to bending or IP due to shear [2,7]. The OOP behaviour of URM walls is often characterised by either one-way or two-way bending of the wall [4]. This behaviour seems to depend mainly on the boundary conditions of the URM panels. Meanwhile, the IP behaviour is characterised by shear failure which is often influenced by wall geometry i.e. the ratio of wall height to its length (H/L) [8].

* Corresponding author.
E-mail address: j.a.dauda@leedsbeckett.ac.uk (J.A. Dauda).

https://doi.org/10.1016/j.engfailanal.2024.108571
Received 30 March 2024; Received in revised form 24 May 2024; Accepted 14 June 2024
Available online 14 June 2024

The assessment of URM walls' IP and OOP response has been extensively studied through experimental, numerical and/or analytical approaches. These approaches enable the assessment of the existing IP or OOP strength of plain URM walls and any improvement as a result of retrofitting actions when a retrofitted masonry wall is tested [9]. Due to advancements in developing various structural retrofitting techniques for URM walls, experimental testing for IP and OOP strength estimations are quite common nowadays, and various testing approaches have been implemented. However, there are discrepancies in the different kinds of experimental approaches used in characterising the IP and OOP behaviour of masonry walls. This is partly due to the unavailability of established uniform testing equipments across all laboratories. In addition, cost, time and capacity limitations among others have led to the emergence of many bespoke testing approaches [1,3] and [6].

This paper provides a systematic review of experimental procedures, focusing on materials and methodologies, to assess the IP and OOP performance of both plain URM walls and those retrofitted with various techniques and materials. By addressing gaps in existing knowledge, the aim is to advance the understanding of URM behaviour under diverse loading conditions. Additionally, the paper aims to compare the approaches commonly employed in IP and OOP testing of masonry walls. The purpose is to understand the details of previous experimental works by critically comparing the (i) wall types/specimen characterisation (i.e. material combination, geometry, specimen quantity and (ii) testing arrangement (i.e. boundary conditions of the URM walls tested, the load application, the testing procedure and the results obtained from the test). The outcome of this review will provide better clarification on testing URM walls and will be instrumental in defining the geometry, boundary conditions, loading and general testing procedure for characterising both the IP and OOP behaviour of masonry walls in future. Additionally, this paper not only aids in simplifying the assessment of the behaviour of masonry structures, acknowledged as a complex construction typology in terms of structural response and mechanical properties [10–12], but also contributes to advancing the field of structural engineering by improving the safety and resilience of masonry infrastructures.

The paper is structured in five different sections with Section 1 providing the background information relevant to this review, the main aim, and the contribution of the review to experimental testing of URM walls. In Section 2, a brief discussion of the structural behaviour of masonry walls is presented while Section 3 presents the detail of the methodology adopted in the systematic review. Section 4 comprises a detailed analysis and discussion of significant findings on masonry wall testing with the conclusion presented in Section 5.

2. Structural behaviour of masonry walls

The behaviour of a masonry wall is typically classified as either in-plane (IP) or out-of-plane (OOP) [7,9]. The response of the URM wall under loading varies significantly to the type of stress induced and it has been widely documented that masonry possesses a significant compressive strength and a low tensile strength [13]. Due to its quasi-brittle nature, URM walls are frequently vulnerable to OOP loading and show a brittle failure [14,15]. For IP loading, masonry tends to demonstrate a more ductile response that is generally governed by a shear failure [14,16] and [17]. Since the focus of this paper is to understand how both behaviours (IP and OOP responses of URM) are experimentally evaluated, both the IP and OOP responses of URM are briefly addressed next.

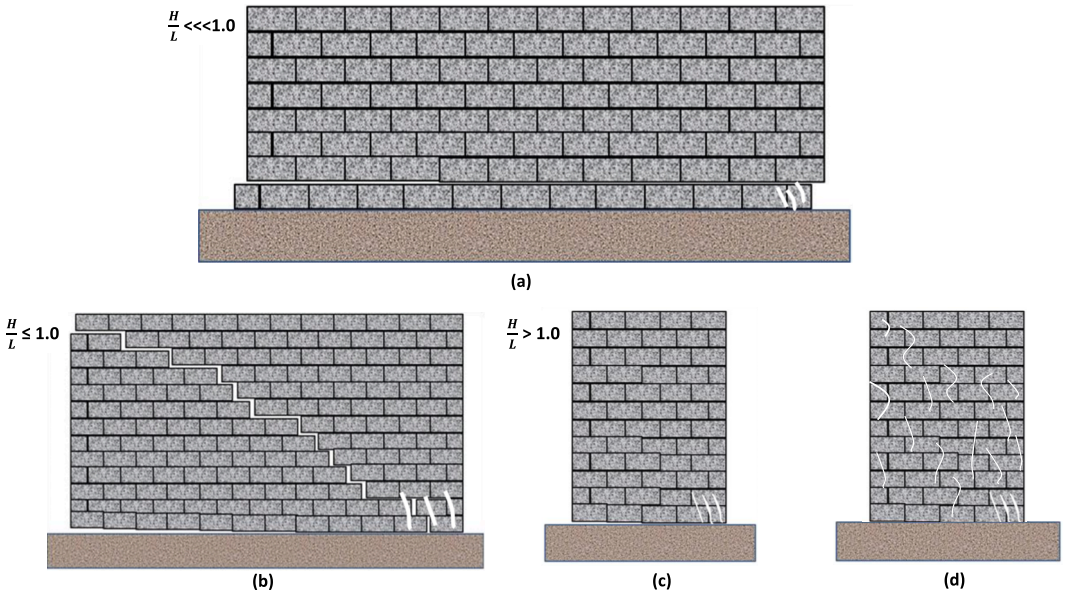

Fig. 1. In-plane failure mode (a) bed-joint sliding, (b) diagonal shear, (c) flexural failure [7] and (d) masonry crushing.

2.1. In-Plane behaviour

The in-plane (IP) structural behaviour of a masonry wall refers to how the wall responds to forces applied within its plane. URM walls exhibit three simple forms of IP failure, as shown in Fig. 1. The wall geometry influences these failure mechanisms i.e. the ratio of wall height to its length (H/L) and layout of joints [18,19]. A shorter wall ($H/L<<1.0$) tends to fail as bed joint sliding shear (Fig. 1**a**), while a short wall ($H/L \leq 1.0$) tends to fail due to diagonal cracking induced by the principal tension perpendicular to diagonal strut (Fig. 1**b**). For walls with ($H/L > 1.0$), flexural failure is the most common failure exhibited (Fig. 1**c**). In addition, IP loading sometime causes compression failure in form of crushing within the masonry section as represented in Fig. 1d. Aside from geometry, the quality of materials used, workmanship during wall construction, inadequate connections, loading types and boundary conditions are some of the factors that influence the IP behaviour of masonry walls. As such, these factors were considered in discussing the outcome of this systematic review in section 4**.**

2.2. Out-of-plane behaviour

The out-of-plane (OOP) behaviour of masonry wall is characterised by either one-way or two-way bending. OOP failure in URM walls primarily occurs due to the absence of elements that can resist tensile forces, failures in connections between perpendicular walls or between walls and diaphragms, the presence of large voids within URM structures, and inadequate connections to transverse structural elements [13,14] and [20]. The OOP behaviour or failure of the URM wall is the most devastating failure mode and causes major hazards in the event of failure [17] and [21]. This assertion corroborated the statement in the BSI (BS EN 1996-1-1) [4] that flexural loading as a result of face-loads on walls in the OOP direction is the worst case. The OOP capacity of the URM walls is influenced by parameters such as wall thickness, slenderness ratio, eccentricity of vertical loading, and wall-to-diaphragm connections [2] and [17]. Meanwhile, the characteristic OOP strength of masonry wall which can be either with the plane of failure parallel or perpendicular to the bed joint as shown in Fig. 2 may be determined by tests following EN 1052-2, ACI and other bespoke testing arrangements that are later reviewed in this paper.

3. Methodology

In an attempt to critically evaluate the experimental investigations that have been carried out so far to understand the IP and OOP behaviour of masonry walls, a systematic literature review (SLR) involving three distinct stages (i.e. identification, collection and analysis of existing relevant literatures) is adopted in this study. This appears an efficient way to establish the existing level of knowledge in a particular subject area and to identify the knowledge gap that can guide future research [22]. Fig. 3 presents the synoptical representation of the SLR conducted in this study starting with literature searches within Scopus which is the largest database for academic research output [23] and complemented by searches of other digital sources such as the Web of Science, Google Scholar, ResearchGate to ensure that the literature searches identify the most relevant publications on the subject of in-plane and out-of-plane testing of masonry walls. This is then followed by data collection and analysis of the returned documents.

3.1. Identification

The Identification (i.e. database search) is the first step of the systematic literature review. Suitable articles are gathered and reviewed in detail. The selection process of articles was achieved by including a combination of keywords, i.e. experiment, testing, masonry, walls, related to the subject matter under review into Scopus. The initial search within ALL (i.e. all fields in Scopus) with the keyword's combination "experimental AND testing AND of AND masonry AND walls'' is very generic and thus returned 10,389 documents. To be more specific, the same keyword combination was searched within TITLE-ABS-KEY (i.e. article title, abstract and keywords) and this returned 927 documents. Thereafter, inclusion and exclusion criteria were imposed on the search to focus the search on the objectives of the study which is to review IP and OOP testing of masonry walls. The provision of the inclusion and

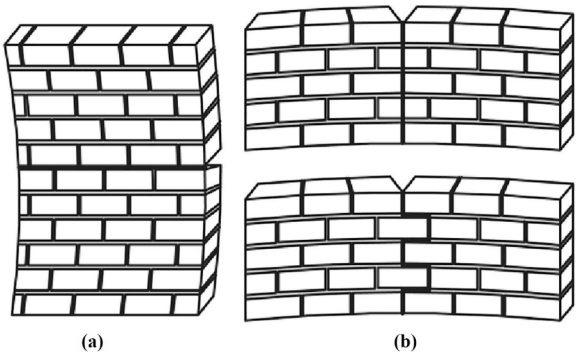

Fig. 2. Out-of-plane failure with failure plane: (a) parallel to bed joints, (b) perpendicular to bed joints [4].

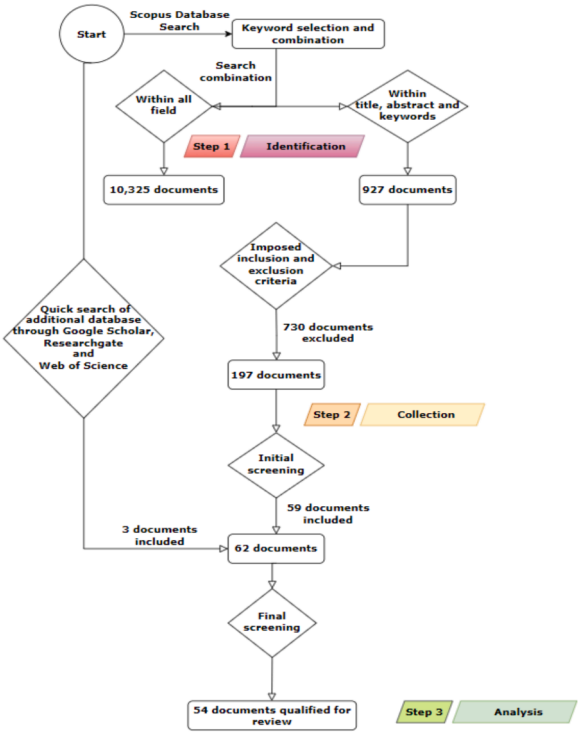

Fig. 3. Overview of the systematic literature review process.

exclusion criteria is very important to restrict the search outcomes to the most relevant literatures [24]. Language and document type are the two main exclusion criteria imposed in this study. So, articles not written in English Languages and conference papers were excluded from the search because most conference articles on experimental studies do not provide details enough for the test to be replicable. Also, in-situ testing and field experimental campaigns were also excluded because they are specific to certain scenarios and difficult to replicate.

For the inclusion criteria, in-plane and out-of-plane were added as compulsory keywords which reduced the number of available documents to 197. In the final step of stage I, an initial screening of the 197 documents returned was carried out and articles focused on retaining walls, infill drilling and earthquakes were removed, making only 59 documents to be retained. Thereafter, a quick search through Google Scholar and Web of Science produced an additional 3 articles which make a total of 62 articles found at the identification stage. The final query string in Scopus is *(TITLE-ABS-KEY (experimental AND testing AND of AND masonry AND walls)) AND (in-plane, AND out-of-plane) AND (LIMIT-TO (LANGUAGE,W "English")) AND (LIMIT-TO (SRCTYPE, "j")) AND (LIMIT-TO (DOCTYPE, "ar")) AND (EXCLUDE (EXACTKEYWORD, "Retaining Walls")) AND (EXCLUDE (EXACTKEYWORD, "Infill Drilling")) AND (EXCLUDE (EXACTKEYWORD, "Earthquakes"))*. This document search was carried out in November 2023.

3.2. Collection

The identification stage is then followed by Stage II, which is the collection stage where the final articles to be reviewed are selected. In this stage, a final screening of the 62 documents was carried out by reading through the abstract and methodology sections of all the 62 articles. After the final screening, 8 articles that do not provide information on either IP testing or out-plane testing on masonry walls were removed, and 54 documents were finally retained for detailed review in subsequent section 4. Fig. 3 presents the details of the flowchart and the corresponding number of articles returned after each step.

4. In-plane and out-of-plane testing of masonry walls

This section presents the significant findings from the review of previous experimental tests on IP and OOP behaviour of masonry walls. Tables 1 and 2 present the details of previous experimental works reporting for each of them, the wall types (geometry and materials combination), boundary conditions of the URM walls tested, the loads applied, testing procedure and the failure modes which were further discussed in sections 4.1 and 4.2.

4.1. In-plane testing of masonry wall – observation from previous studies

The critical evaluation of previous experimental studies that have been conducted to understand the IP behaviour of masonry walls has been carried out and the key observations from the review are summarised in Table 1. Thereafter, the deductions form the systematic review are discussed in sections 4.1.1 for wall types and 4.1.2 for testing arrangement in line with the objectives listed in section 1.

4.1.1. Overview of wall types for IP testing – material, geometry and quantity of specimen

The choice of materials, geometry and the number of specimens to be tested for the evaluation of the IP behaviour of masonry walls is crucial when planning an experimental study because masonry structures exhibit complex and heterogeneous behaviour due to variations in materials, construction techniques, and environmental factors [9,21,40]. Therefore, it is important to select appropriate materials and geometry for the specimens to ensure that the experimental results closely mimic real-world scenarios, leading to more accurate and representative data. The observations from the review of past studies are discussed in terms of the specimen wall types based on materials combination, geometry and quantity tested as follows:

Materials Combination

Most of the reviewed articles except [25] and [36] indicate a material combination with stronger unit-weak mortar joints. These combinations often manifest in older masonry structures, where the individual masonry units possess higher strength than the mortar joints binding them together. The material selection for IP testing will depend on the goal of the study. Where the motive is to develop a retrofit technique like in most of the cases reviewed, it is appropriate to select a material combination that represents one commonly found in old buildings (stronger unit and weaker mortar joints). Where the aim is to understand the performance of newly intended masonry materials such as 3D printed masonry blocks [27] and mortarless concrete blocks [38], various combinations can be tested to ensure an optimum material combination is obtained. This will facilitate a better understanding of the behaviour of historic masonry structures and aid in the development of appropriate restoration and retrofit strategies. The basic influence of this in the failure pattern is that the failure always occurs in the weaker of the masonry unit and mortar joint as observed in the results of the experiment studies reviewed. This is because when a load is applied to the wall specimens, stress is distributed throughout the units and the mortar joints and the weaker of the two fails first. For instance, the lower strength of the mortar, 4.09 N/mm^2 in [20] compared to 5.68 N/mm^2 [32] means that it can withstand less stress and have a lower diagonal failure load of 170 kN compared to that of [32] with a load capacity of 189 kN. As a result, the overall capacity of the structure to bear loads is limited by the strength of the mortar. It is important to carefully consider both unit strength and mortar strength when designing and constructing new load-bearing masonry structures or when retrofitting existing ones. It is worth mentioning that the comparison of masonry strength is not consistent because the complexities that arise from variations in workmanship and testing setups make it difficult to ascertain a direct correlation.

Geometry of Masonry Wall Specimen

The geometry of the masonry wall specimen used in IP experiments varies depending on the testing arrangement as discussed later in the section 4.1.2. However, the specimen geometry is predominantly square in shape except when testing under vertical compression test (axial-compression loading) or IP load on the side instead of diagonal loading where the sections have slenderness ratio (h/l) $>$ 1.0 as observed in [28,30,37–39]. The comparison of various experimental results aimed at investigating the effect of specimen size on structural behaviour reveals intriguing insights. In diagonal testing, specimens exhibited a wide range of dimensions, with minimum sizes measuring 200x200x50 mm^3 and maximum sizes stretching to 1270x1270x311 mm^3. Notably, an increase in specimen thickness emerged as a key factor influencing diagonal shear strength. This outcome was attributed to the fact that thicker specimens displayed enhanced resistance of the joint to failure and since the failure mostly occurred in the joint, this leads to stronger masonry. Unsurprisingly, the axial load tests highlighted a similar trend with an increase in slenderness ratio leading to a decrease in wall capacity. Moreso, the review revealed that the application of interlocking among bricks contributes to the shear strength of the masonry specimen.

Although wall type i.e both the geometry and material combination of the specimen are key determinants of the IP behaviour, this review revealed that there are challenges in establishing a robust relationship between mortar strength, specimen geometry and shear stress. This complexity arises from variations in workmanship and testing setups, making it difficult to ascertain a direct correlation. Unfortunately, despite the valuable insights garnered, the existing experimental data falls short of enabling a comprehensive evaluation of the influence of specimen size on the shear strength. Additionally, attempts to correlate results from small-scale tests to larger specimens remain elusive. This highlights a critical gap in our understanding, emphasising the need for further comprehensive experimentation to fully understand the influence of thickness, slenderness ratio, and interlocking mechanisms on the shear strength of masonry specimens for structural applications.

Number of Specimens

In IP experiments, the number of specimens in a single group is often odd, typically three. This odd number is chosen to allow for more meaningful statistical analysis and robust conclusions. However, an exception is made when the first two results are in agreement [30,32,37–39], In such cases, the third specimen might not be necessary to validate the behaviour of the masonry structure. This approach optimises resources while maintaining scientific rigour. The outcome of the review has confirmed that researchers often made this adjustment for more efficient use of resources without compromising the reliability of the test outcomes.

4.1.2. Testing arrangement for IP testing – boundary condition, loading procedure and rate

The arrangement of the testing and loading configuration leads to varying stress distributions and failure mechanisms in masonry specimens. The review presented reveals four distinct testing arrangements for IP-testing of masonry specimens as shown in Fig. 4 with

their corresponding failure pattern. The most adopted arrangement for IP testing of masonry specimens is the diagonal loading of the specimen in a vertical position (Fig. 4**a**), which is simply referred to as IP in Table 1. The application of axial compression loading on the top of the specimen (IP-Axial) testing arrangement represented in Fig. 4**b** is the second most common testing arrangement for the evaluation of IP behaviour of masonry specimens. Occasionally, two other testing arrangements which are diagonal loading of the specimen in horizontal position IP-Hor in Fig. 4**c**, and application of load on the side of the specimen (IP- Side Axial in Fig. 4**d**) are used as observed in [25] and [36]. The subsequent section presents the discussion on the boundary condition, loading procedures and rate, and their corresponding influence on the failure mechanism of masonry specimens under IP loading.

Boundary Condition

The boundary conditions in masonry testing play a critical role in determining the behaviour and failure patterns of the specimens under different loading conditions. In the context of the diagonal compression test (in-plane), the diagonal loading shoe creates the boundary condition and specific loading path that induces diagonal compression forces. This boundary condition ensures that the failure pattern observed in all cases of IP is the same and majorly described as a diagonal crack in a stair-stepped shape in the head and bed joints as previously shown in Fig. 4**a** [25–39]. The consistency in the diagonal failure pattern observed in the reviewed tests suggests that the diagonal compression test primarily tests the material's ability to withstand diagonal forces and shearing stresses. Meanwhile, the boundary condition applied in the axial compression test (IP-Axial) which involves placing the specimens on a hard resistant floor with a precompression load on top before imposing the axial load [30,38] mimics real-world scenarios where structures are subjected to axial loads. This test arrangement produces a failure pattern that is characterised by vertical cracks on both faces of the specimen and later separation of wythes as shown in Fig. 4**b**. The vertical splitting of face shells and cracking in the web-shells that occur in the axial compression test can be attributed to the boundary condition and the specific loading path which is a compressive force along the height of the specimen. The observed failure pattern of the IP-Axial testing configuration indicates that this test is more focused on assessing the material's ability to withstand axial forces and the resulting deformation, which is different from the shear force in the diagonal testing. The values of stress and load capacity differ between the diagonal and axial compression tests as observed in [30] where a maximum load of 396KN was reported as failure load for IP testing arrangement in comparison to 2163 KN for IP-Axial. The lower value of the load capacity of IP is attributed to the load path which is majorly on the joint unlike in the IP-Axial where the load is transferred to the unit first. So, when making comparisons for the strength of masonry configuration, consistency is crucial for accurate material characterisation and testing arrangement to allow researchers and engineers to make meaningful comparisons between different materials or structural arrangements.

Loading Procedure and Rate

Loading procedures and application rates have considerable influence over the behaviour, failure load, and ultimate failure patterns of the tested masonry walls. From the previous studies, two principal methods of load application emerged these are load control and displacement control methods. In load-controlled testing such as [26], the masonry specimen is subjected to specific loads and the corresponding displacement is recorded. Meanwhile displacement-controlled testing such as [35,29] and [33] focuses on attaining certain deformations and measuring the corresponding loads needed to achieve those deformations. However, the challenges facing experimental testing as observed from the reviewed tests is the lack of consistency in the loading procedure or loading rate across all the reviewed articles. In fact, many of the reviewed articles did not indicate any specific standards or codes that were followed in conducting the test. Even where the studies claimed to use ASTM E519 such as [31] and [32], the studies refrained from providing explicit loading rates and opted for vague descriptions such as "gradual" loading. This absence of standardised rates complicates the direct comparison of results across different studies, potentially obscuring a coherent understanding of the impact of loading rates on the strength of masonry specimens.

Despite this inconsistency in loading rate and, consequently, the variation in failure load, noticeable patterns emerged regarding the effects of loading rates on failure behaviour. The key observation from the review is that tests conducted at lower loading rates generally yield higher failure loads. This phenomenon can be attributed to the gradual deformation of the masonry specimen over an extended period. Such loading conditions afford the masonry units and mortar joints ample time to redistribute stresses and mitigate stress concentrations, leading to more ductile response and, consequently, an enhanced load-carrying capacity. Conversely, tests employing higher loading rates tend to display more abrupt, brittle failure behaviour. The rapid application of load introduces higher stress concentrations within the masonry specimen which can trigger localised failure and precipitate a sudden collapse mechanism. This brittle behaviour is often characterised by a lack of substantial warning signs or significant deformations prior to failure.

4.2. Out-of-plane testing of masonry wall – observation from previous studies

Table 2 presents the general overview of how the selected studies have conducted out-of-plane (OOP) testing on masonry walls. Similar to the discussion presented in section 4.1 for the IP testing, the review looked critically at understanding the specimen characterisation and testing arrangement for OOP and key findings are discussed in sections 4.2.1 and 4.2.2.

4.2.1. Overview of wall types for OOP testing – material, geometry and quantity

The observation of the materials combination and the number of specimens tested in the evaluation of out-of-plane (OOP) behaviour are notably similar to those employed in the investigation of in-plane (IP) behaviour, as expounded upon in the section 4.1. This connection underscores the natural form in which masonry structures are, which is mostly a combination of stronger units and weaker joints. In all the reviewed studies, only [48] and [45] reported combinations of stronger mortar-weaker units with mortar strength values (6.81 N/mm^2 and 39.3 N/mm^2, respectively) that exceeded their corresponding individual unit strengths of 6.31 N/mm^2 and 14.71 N/mm^2, respectively. Also, the number of specimens tested is always odd (i.e. 3 per group) except in a few cases where

the first two specimens are deemed to have produced the same results such as [52] and [63]. One standout study [41] evaluates 18 full-scale masonry veneer wall systems under OOP loading to probabilistically assess behaviour. In terms of geometry, segmented specimens focussing on smaller sections or panels of masonry are the most commonly tested specimens in OOP testing. The main reason for using this smaller section is to allow more controlled testing and is often used when studying specific details or retrofitting techniques [5]. From the reviewed studies, different sizes of masonry walls ranging from 500 x 500 x 75 mm to 4100 x 1150 x 230 mm were tested. The most important thing is to ensure that the selected geometry for OOP testing aligns with the specific objectives of the study and the characteristics of the masonry structure being investigated.

The analysis of the reviewed experimental studies revealed that there is a clear relationship between the thickness of the specimen and the OOP load-carrying capacity of the masonry specimen. The displacement experienced by the specimen prior to failure also exhibits a positive correlation with thickness. This trend underscores the importance of thickness in governing the OOP behaviour of masonry walls and highlights its role in influencing structural integrity. However, the concern about the complexities in correlating geometric impacts on the strength of masonry specimens due to varying workmanship and testing conditions still exists as observed in the IP-testing. These further ascertain the intricacies surrounding masonry wall behaviour under OOP loading and necessitate further research.

4.2.2. Testing arrangement for OOP testing – boundary condition, loading procedure and rate

The boundary conditions refer to the way the wall is supported or restrained at its edges or corners [17] during testing. Different boundary conditions can lead to varying behaviours and responses of the wall under load because boundary conditions play significant roles in determining the flexural capacity and displacement of a masonry wall under OOP loading. The review shows that OOP testing is conducted using any simply supported boundaries, fixed or restrained boundaries, and partial restraints boundaries (Fig. 5). The most common boundary conditions in testing specimens under OOP loading involve configuring the top and bottom edges with the freedom to rotate while fixing OOP displacements. This configuration, known as simply supported boundaries, is characterised by the bottom support (Support-BOT) being either free (BOT1), and the top support (Support-Top) being either free or TOP1. Essentially, the base of the wall is constrained against axial displacements, while the top remains free for axial load application. Simply supported boundaries allow for the free rotation and deflection of the wall, promoting a more ductile behaviour but potentially leading to larger deflections. However, in some instances, as noted in references [54,55] and [56], fixed or restrained boundaries are imposed on the wall. Walls with fixed or restrained boundaries are less prone to rotation and deformation, resulting in higher flexural capacity. This restraint, however, also translates to higher stresses in the wall and a more brittle behaviour when the wall's capacity is exceeded. In certain cases, walls may feature partial restraints at specific edges or corners [64], introducing complexities in interactions between different boundary conditions. This complexity can result in differential deformations and potential cracking, with the behaviour of such walls contingent on the distribution and nature of these partial restraints. The adoption of simply supported boundaries is influenced by their ability to provide a balance between ductility and controllability, their versatility in experimental setups, their established presence in literature, ease of implementation, their capacity for studying differential deformations, and their suitability for comparative studies.

Loading Procedure and Rate

Inconsistent loading applications and rates across various studies, similar to the observations in IP testing, hinder the ability to compare outcomes. This inconsistency arises from the absence of reference to testing standards or guidelines, even when studies claim to adhere to them. For example, studies [2] and [40] both claimed adherence to ASTM E72, but one reported a loading rate of 1 kN/min, while the other used a gradual increment. This variation influences test outcomes, as applying a load at a known rate allows for a more predictable and controlled response from the wall, capturing real behaviour and failure load accurately. In OOP testing, the predominant load applications are point loads (four-point loading or three-point loading) and uniformly distributed loading (UDL) on wall specimens. Point load applications involve one or two lines of force simulated by steel profiles, while UDL is applied using inflatable airbags. The most common method is the application of point loads through line loads. However, it has been previously argued in 2006 that this type of loading does not accurately represent the OOP behaviour of the wall in both directions and does not align with real-world loading scenarios [65]. Despite this critique, it remains the most widely used method in the field of masonry testing, demonstrating a stagnancy in testing approaches over 23 years. However, studies such as [17], and [41] applied uniform inward and outward out-of-plane loading using airbags to replicate the wind loading scenario. For each loading type, one specimen underwent semi-cyclic loading to assess whether the monotonic loading could capture the overall behaviour of the cyclic response.

Despite challenges, a consistent theme in these studies is the observed failure pattern in masonry walls subjected to OOP loading. Cracks consistently form at a single joint near the mid-height of the walls across various experimental setups as shown in Fig. 5. This recurring failure mode offers valuable insights into critical weak points within masonry walls under OOP loads. However, challenges persist in establishing correlations between geometric factors and strength due to diverse testing arrangements and loading rates across studies. These variations impede direct comparisons and comprehensive analyses, making it difficult to draw generalised conclusions about the influence of geometry, support condition, and loading rate on OOP strength.

5. Final remarks

This study addresses a systematic literature review of 54 scientific articles related to IP or OOP testing of masonry walls spanning from 2010. The review provided an understanding of the challenges and patterns associated with the crucial aspect of evaluating the structural performance of masonry walls. The review outcomes emphasised the intricate interplay between both the IP and OOP performances and various influencing factors such as specimen material properties, geometry, boundary conditions, loading procedures and failure patterns. Of the influencing factors, only material combination and failure patterns are consistent across several

Table 1
Overview of in-plane experimental studies.

DLS- *diagonal loading shoe at the top and bottom diagonal*; **BOT1**-*bottom of the specimen bonded to concrete beam with steel roller underneath the beam*; **BOT2**-*bottom of the specimen bonded to concrete beam on strong floor*; ***TOP1***-*pre-compression load applied on top of specimen;* ***TOP2***- *Top of the specimen restrained on both side;* **SB3-** *post-tensioned rebar on both side like column;* **SB4-** *returning wall on both side rest against strong resistance wall;* **LT1**- *four-point loading with two loading points each @ approx. span/3;* **LT2**- *four-point loading with two main loading points each @ approx. span/3 and multiple loading points @ span/6*

REF	Type	Brick (N/mm^2)	Mortar (N/mm^2)	Geometry (h × l × t in mm)	Slenderness ratio (h/l)	Qty	Standard	Support-Bottom	Support-Top	Support-Back	Loading Type	Loading Rate	Instrument	Measured	Plot	Estimated-results	Failure Mode
[25]	IP-Side	11.8	14.26	1910 × 2200 × 70	0.9	4	n/a	BOT1	TOP1	SB3	in-plane load on the side	gradually	load cell and LVDTs	load and displacement	load – displacement	ultimate load, strength, and stiffness	cracks along the diagonal top of the wall to the spandrel
[26]	IP	24	22	1145 × 1220 × 92	0.9	3	ASTM E519	DLS	Free	Free	diagonal loading	gradually	load cell and LVDTs	load and displacement	load – displacement	cracking load and displacement	diagonal crack in a stair-stepped shape in the head and bed joints
[27]	IP	23.3	6.73	200 × 200 × 50	1	3	ASTM E519-20	DLS	Free	Free	diagonal loading	gradually	load cell and LVDTs	load and displacement	n/a	peak shear stress and strain	surface cracking of blocks that later spread along the diagonal units and joint of prisms
[28]	IP	17.99	2.19	1270 × 1270 × 311	1	5	ASTM 519 and LUMB6 of RILEM	DLS	Free	Free	diagonal loading	0.5 mm/min	pressure transducers and LVDTs	load and displacement	load–displacement	capacity in terms of stress and strain	cracks along the diagonal units and joints across prisms
[29]	IP-Side	14.83	4.59	1800 × 1800 × 340	1	3	n/a	BOT2	TOP1	Free	in-plane load on the side	0.2 mm/s	pressure transducers and LVDTs	load and displacement	load–displacement	maximum load, stiffness, and dissipated energy	formation of a stair-stepped diagonal crack in both mortar bed joints and bricks
[30]	IP	30.5	4.78	1200 × 1200 × 250	1	2	ASTM 519	DLS	Free	Free	diagonal loading	1.0 KN/s	load cell and LVDTs	load and displacement	stress–strain	load capacity, modulus of elasticity	diagonal crack in both mortar bed joints and bricks
[31]	IP	13.69	3.02	650 × 650 × 250	1	6	ASTM E 519–02	DLS	Free	Free	diagonal loading	gradually	load cell and LVDTs	load and displacement	shear stress –shear strain	shear modulus	stair-stepped diagonal crack in both mortar bed joints and bricks
[32]	IP	24.03	5.68	1200 × 1200 × 250	1	2	ASTM E519	DLS	Free	Free	diagonal loading	gradually	load cell and LVDTs	load and displacement	shear stress –shear strain	shear modulus	diagonal cracks in step-like pattern
[33]	IP	8	6.6	1000 × 1000 × 250	1	3	ASTM E 519 and RILEM TC-76	DLS	Free	Free	diagonal loading	0.15 mm/min	load cell, LVDTs and strain gauge	load and displacement	shear stress – shear strain	stiffness, shear strength and shear modulus	vertical cracks appeared at the lateral sides of the specimens

(*continued on next page*)

Table 1 (*continued*)

DLS- *diagonal loading shoe at the top and bottom diagonal*; **BOT1**-*bottom of the specimen bonded to concrete beam with steel roller underneath the beam*; **BOT2**-*bottom of the specimen bonded to concrete beam on strong floor*; ***TOP1***-*pre-compression load applied on top of specimen;* ***TOP2***- *Top of the specimen restrained on both side;* **SB3-** *post-tensioned rebar on both side like column;* **SB4-** *returning wall on both side rest against strong resistance wall;* **LT1**- *four-point loading with two loading points each @ approx. span/3;* **LT2**- *four-point loading with two main loading points each @ approx. span/3 and multiple loading points @ span/6*

REF	Type	Brick (N/mm^2)	Mortar (N/mm^2)	Geometry (h × l × t in mm)	Slenderness ratio (h/l)	Qty	Standard	Support-Bottom	Support-Top	Support-Back	Loading Type	Loading Rate	Instrument	Measured	Plot	Estimated-results	Failure Mode
[20]	IP	44	4.09	1160 × 1160 × 250	1	3	n/a	DLS	Free	Free	diagonal loading	gradually	transducers, potentiometer	load and displacement	load – strain	cracking load and displacement	cracks along the diagonal units and joints across prisms
[34]	IP	38.75	2.69	1200 × 1200 × 240	1	6	ASTM 519	DLS	Free	Free	diagonal loading	gradually	load cell and LVDTs	load and displacement	shear stress – angular strain	shear strength and shear modulus	cracks along the diagonal units and joints across prisms
[35]	IP	25.4	13.8	860 × 860 × 250	1	3	ASTM 519—10	DLS	Free	Free	diagonal loading	0.005 mm/s	load cell and LVDTs	load and displacement	stress–strain	compressive strength, modulus of elasticity and energy absorption	cracks along the diagonal units and joint of prisms
[35]	IP – Axial	25.4	13.8	760 × 760 × 250	1	3	EN 1052–1	Free	Free	Free	axial-compression load	0.005 mm/s	load cell and LVDTs	load and displacement	stress–strain	compressive strength, modulus of elasticity and energy absorption	vertical cracks on both faces of the specimen and later separation of wythes
[36]	IP-HOR	8.4	12.98	600 × 600 × 120	1	6	ASTM 519–15	DLS	Free	SB1	diagonal loading horizontal	gradually	load cell and LVDTs	load and displacement	load – displacement	ductility and energy dissipation	cracks along the diagonal units and joints across prisms
[30]	IP-Axial	30.5	4.78	1200 × 1000 × 250	1.2	2	n/a	BOT2	Free	Free	axial-compression load	2.0 kN/s	load cell and LVDTs	load and displacement	stress–strain	load capacity, modulus of elasticity	vertical cracks on both faces of the specimen and later separation of wythes
[37]	IP-Axial	H14	3.4	800 × 600 × 190	1.3	2	n/a	Free	TOP1	Free	axial-compression load	gradually	load cell, LVDTs and laser beam	load and displacement	load – displacement	axial capacity, shear stress and strain	vertical splitting of face shells, and cracking in the web-shells

(*continued on next page*)

Table 1 (*continued*)

DLS- *diagonal loading shoe at the top and bottom diagonal*; **BOT1**-*bottom of the specimen bonded to concrete beam with steel roller underneath the beam*; **BOT2**-*bottom of the specimen bonded to concrete beam on strong floor*; ***TOP1***-*pre-compression load applied on top of specimen;* ***TOP2***- *Top of the specimen restrained on both side;* **SB3-** *post-tensioned rebar on both side like column;* **SB4-** *returning wall on both side rest against strong resistance wall;* **LT1**- *four-point loading with two loading points each @ approx. span/3;* **LT2**- *four-point loading with two main loading points each @ approx. span/3 and multiple loading points @ span/6*

REF	Type	Brick (N/mm^2)	Mortar (N/mm^2)	Geometry (h × l × t in mm)	Slenderness ratio (h/l)	Qty	Standard	Support-Bottom	Support-Top	Support-Back	Loading Type	Loading Rate	Instrument	Measured	Plot	Estimated-results	Failure Mode
[38]	IP-Axial	H27.9 and H18.5	n/a	800 × 600 × 190	1.3	4	n/a	Free	Free	Free	axial-compression load	2 mm/min	load cell and LVDTs	load and displacement	load – displacement	peak load, stress capacity and strain	vertical splitting of face shells, and cracking in the web-shells
[38]	IP-Axial	H27.9 and H18.4	n/a	1400 × 600 × 190	2.3	4	n/a	Free	free	Free	axial-compression load	1 mm/min	load cell and LVDTs	load and displacement	load – displacement	peak load, stress capacity and strain	vertical splitting of face shells, and cracking in the web-shells
[39]	IP-Axial	H15	4.4	1400 × 600 × 190	2.3	2	n/a	Free	TOP2	Free	axial-compression load	gradually	load cell, LVDTs and laser beam	load and displacement	load – displacement	axial capacity, shear stress and strain	vertical splitting of face shells, and cracking in the web-shells
[28]	IP-Axial	H16	5.4	2400 × 600 × 190	4	3	n/a	Free	TOP2	Free	axial-compression load	gradually	load cell, LVDTs and laser beam	load and displacement	load – displacement	axial capacity, shear stress and strain	vertical splitting of face shells, and cracking in the web-shells
[39]	IP-Tilting	–	n/a	1485 × 2000 × 110	0.74	7	n/a	Free- dry jointed wall on tilting table	n/a	n/a	tilting table movement	0.83∘/s u	inclinometer	collapse and angle of inclination	n/a	shear capacity	typically characterised by the overturning of the pillars

IIP: diagonal loading of the specimen in a vertical position; IP-Axial: compression loading on the top of the specimen (compression test); IP-Hor: diagonal loading of the specimen in horizontal position; IP-Side Axial: load on the side of the specimen.

Table 2
Overview of Out-of-Plane Experimental Studies.

BOT1-*bottom of the specimen bonded to concrete beam with steel roller underneath the beam*; **BOT2**-*bottom of the specimen bonded to concrete beam on the strong floor*; **BOT3**-*bottom of the specimen bonded to concrete beam on strong floor and restrained on both side;* ***TOP1***-*pre-compression load applied on top of specimen;* ***TOP2***- *Top of the specimen restrained on both side;* **SB1**- *specimen tested with rollers at the back of the top and bottom courses of the specimen (pinned–pinned);* **SB2**- *specimen tested with rectangular pipes at the back of the top and bottom courses of the specimen (pinned–pinned);* **SB3**- *post-tensioned rebar on both side like column;* **SB4**- *returning wall on both side rest against strong resistance wall;* **LT1**- *four-point loading with two loading points each @ approx. span/3;* **LT2**- *four-point loading with two main loading points each @ approx. span/3 and multiple loading points @ span/6*

REF	Type	Brick (N/mm^2)	Mortar (N/mm^2)	Geometry (h × l × t in mm)	Slenderness ratio (h/l)	Qty	Standard	Support-Bottom	Support-Top	Support-Back	Loading Type	Loading Rate	Instrument	Measured	Plot	Estimated-results	Failure Mode
[41]	OOP	25.2	3.1	2398 × 2390 × 110	1	18	n/a	BOT1	free	SB2	UDL via inflatable airbag	gradually	gauge, LVDTs, potentiometer	pressure, deflection and displacement	Pressure – displacement	cracking load in the form of pressure, maximum deflection	cracks at a single joint near mid-height
[2]	OOP	87.9	7.1	1115 × 1115 × 215	1	6	ASTM E72-15	BOT1	TOP1	SB1	four-point loading	1 kN/min	load cell and LVDTs	load and displacement	load – displacement	toughness, maximum load, displacement and energy dissipation	cracking of joints on the tension face and crushing of interlocking blocks at the compression face
[42]	OOP	24	22	1422 × 1220 × 92	1.2	3	N/A	BOT2	free	SB2	UDL using inflatable airbag	0.1 psi/min	load cell and LVDTs	displacement and load	load – displacement	maximum moment, pressure	cracks located at the mortar joints near the mid-height
[43]	OOP	n/a	10.43	1050 × 790 × 115	1.3	6	n/a	free	free	SB1	four-point loading	gradually	Load gauge and deflection gauges	load and deflection	bending moment – deflection	cracking load and displacement, flexural capacity and bending moment	cracks at the interface between the ceramic units and the mortar
[30]	OOP	30.5	4.78	1200 × 800 × 250	1.5	6	n/a	free	free	SB1	three-point loading	100 N/sec	load cell and LVDTs	load and displacement	load – displacement	peak load and displacements	separation at the interface between the horizontal mortar joint and brick unit
[44]	OOP	25.6	12.5	3800 × 2600 × 140	1.5	3	n/a	B0T2	TOP1	SB1	horizontal line-load on top of the wall	gradually	load cell and LVDTs	load and displacement	load – displacement	peak load, peak lateral displacement, and energy dissipation	flexural cracks accompanied by the onset of face shell spalling at the wall toes
[45]	OOP	14.71	39.3	1422 × 812 × 203	1.8	3	ASTM E58	BOT1	free	SB1	four-point loading	gradually	load cell and LVDTs	load and displacement	load – displacement	peak load and deflection	cracking of joints facing the tension face of the unit and then extended to

(*continued on next page*)

Table 2 (*continued*)

BOT1-*bottom of the specimen bonded to concrete beam with steel roller underneath the beam*; **BOT2**-*bottom of the specimen bonded to concrete beam on the strong floor*; **BOT3**-*bottom of the specimen bonded to concrete beam on strong floor and restrained on both side;* ***TOP1***-*pre-compression load applied on top of specimen;* ***TOP2***- *Top of the specimen restrained on both side;* **SB1**- *specimen tested with rollers at the back of the top and bottom courses of the specimen (pinned–pinned);* **SB2**- *specimen tested with rectangular pipes at the back of the top and bottom courses of the specimen (pinned–pinned);* **SB3**- *post-tensioned rebar on both side like column;* **SB4**- *returning wall on both side rest against strong resistance wall;* **LT1**- *four-point loading with two loading points each @ approx. span/3;* **LT2**- *four-point loading with two main loading points each @ approx. span/3 and multiple loading points @ span/6*

REF	Type	Brick (N/mm^2)	Mortar (N/mm^2)	Geometry (h × l × t in mm)	Slenderness ratio (h/l)	Qty	Standard	Support-Bottom	Support-Top	Support-Back	Loading Type	Loading Rate	Instrument	Measured	Plot	Estimated-results	Failure Mode
[46]	OOP	H27.9	n/a	1200 × 600 × 190	2	3	n/a	BOT1	free	SB1	four-point loading	1 mm/min	load cell, laser sensor and DIC	load and deflection	Load −displacement	cracking load and displacement, flexural capacity, modulus of rupture	surrounding units at tension face opening of dry-joint on the tension face and crushing of interlocking blocks at the compression face
[47]	OOP	7.76	0.85	2400 × 1200 × 150	2	2	Masonry Standards Joint Committee (MSJC)-11	BOT1	free	SB1	four-point loading	gradually	load cell and LVDTs	load, displacement	load −displacement	flexural strength	horizontal cracking in the grout cores in dry stacked joints initiated at low force levels
[48]	OOP	6.31	6.81	1235 × 590 × 145	2.1	3	BS 5628	free	TOP1	SB1	four-point loading	gradually	load cell and LVDTs	load and displacement	Load − displacement	peak load, displacement and flexural strength	cracking of joints on the tension face and crushing of interlocking blocks at the compression face
[49]	OOP	43.83	1.28	1600 × 700 × 350	2.3	6	n/a	BOT2	free	SB4	UDL using inflatable airbag	incremental	load cells and transducers	load and displacement	load − displacement	cracking load and displacement	overturning of the wall due to the anchorage at the bottom
[50]	OOP	26.16	14.75	1225 × 485 × 230	2.5	4	ASTM E518/ E518M-15	free	free	SB1	four-point loading	gradually	load cell and LVDTs	load and displacement	load − displacement	stiffness and ductility capacity	cracking of joints on the tension face and crushing of units at the compression face
[51]	OOP	8.8	3.2	3300 × 1170 × 150	2.8	3	ASTM C1072	BOT2	TOP1	free	UDL using inflatable airbag	gradually	Pressure transducers and LVDTs	Load and displacement	load − displacement	cracking load and displacement	crack at the wall base, and the horizontal joint at

(*continued on next page*)

Table 2 (*continued*)

BOT1-*bottom of the specimen bonded to concrete beam with steel roller underneath the beam*; **BOT2**-*bottom of the specimen bonded to concrete beam on the strong floor*; **BOT3**-*bottom of the specimen bonded to concrete beam on strong floor and restrained on both side;* ***TOP1****-pre-compression load applied on top of specimen;* ***TOP2-*** *Top of the specimen restrained on both side;* **SB1-** *specimen tested with rollers at the back of the top and bottom courses of the specimen (pinned–pinned);* **SB2-** *specimen tested with rectangular pipes at the back of the top and bottom courses of the specimen (pinned–pinned);* **SB3-** *post-tensioned rebar on both side like column;* **SB4-** *returning wall on both side rest against strong resistance wall;* **LT1**- *four-point loading with two loading points each @ approx. span/3;* **LT2**- *four-point loading with two main loading points each @ approx. span/3 and multiple loading points @ span/6*

REF	Type	Brick (N/mm^2)	Mortar (N/mm^2)	Geometry (h × l × t in mm)	Slenderness ratio (h/l)	Qty	Standard	Support-Bottom	Support-Top	Support-Back	Loading Type	Loading Rate	Instrument	Measured	Plot	Estimated-results	Failure Mode
[52]	OOP	44	3.1	3000 × 1000 × 250	3	2	n/a	BOT1	free	SB1	four-point loading	gradually	pressure transducers and LVDTs	load and displacement	load – displacement	moment, load capacity and displacement	approximately mid-height cracks at the tensed face of the samples (the front) at about wall mid-height
[53]	OOP	87.9	7.1	665 × 215 × 65	3.1	3	ASTM E72-15	BOT1	TOP1	SB1	four-point loading	gradually	load cell and LVDTs	load and displacement	load – displacement	flexural strength and maximum displacement	cracks at a single joint near mid-height
[40]	OOP	39.4	1.4	3670 × 1200 × 220	3.1	3	n/a	BOT3	TOP2	free	UDL using inflatable airbag	gradually	transducers and load cell	pressure and displacement	load – displacement	failure load and displacements	cracking of joints facing the tension face of the specimen above mid-point
[54]	OOP	35.5	13.9	3750 × 1200 × 215	3.1	3	ASTM E72-15	BOT2	TOP1	SB2	UDL using inflatable airbag	gradually	load cell and LVDTs	Load and displacement	load – displacement	maximum capacity	horizontal crack near the mid-height of the wall
[55]	OOP	21.4	0.9	4100 × 1150 × 230	3.6	3	ASTM E72-15	BOT3	TOP2	free	UDL using inflatable airbag	gradually	Load cell and transducers	load and displacement	load – displacement	failure load and displacements	cracking of joints t the specimen tension face
[56]	OOP	39.5	2.1	4100 × 1150 × 230	3.6	4	n/a	BOT2	TOP2	free	UDL using inflatable airbag	gradually	load cell and LVDTs	displacement and load	load – displacement	load capacity, deformation and stiffness	horizontal cracks through the mortar joints up the wall height
[57]	OOP	39.5	8.8	4100 × 1150 × 230	3.6	3	n/a	BOT2	TOP1	free	UDL using inflatable airbag	gradually	load cell and LVDTs	displacement and load	load – displacement	maximum moment, pressure	horizontal cracks through the mortar joints up the wall height
[46]	OOP	H18.4	n/a	2400 × 600 × 190	4	3	n/a	BOT1	TOP1	SB1	four-point loading	2 mm/min	load cell, laser sensor and DIC	load and deflection	Load vs. displacement	cracking load and displacement, flexural capacity, modulus of rupture	opening of dry-joint on the tension face and crushing of interlocking blocks at the compression face
[58]	OOP-HOR	8.2	5	500 × 500 × 75	1	4	ASTM E518	free	free	SB1	four-point loading	0.3 mm/sec	load cell and LVDTs	load and displacement	load – displacement	strength, stiffness	cracks at joint near mid-height to split specimen into two
[59]	OOP-HOR	35	8.9	1980 × 1800 × 400	1.1	3	n/a	free	free	SB2	Four-point loading	1.5KN increment	Load cell and transducers	maximum load and cracking displacement	n/a	failure load and displacements	cracks at the joint near the load point to split the specimen into two

(*continued on next page*)

Table 2 (*continued*)

BOT1-*bottom of the specimen bonded to concrete beam with steel roller underneath the beam*; **BOT2**-*bottom of the specimen bonded to concrete beam on the strong floor*; **BOT3**-*bottom of the specimen bonded to concrete beam on strong floor and restrained on both side;* ***TOP1***-*pre-compression load applied on top of specimen;* ***TOP2***- *Top of the specimen restrained on both side;* **SB1**- *specimen tested with rollers at the back of the top and bottom courses of the specimen (pinned–pinned);* **SB2**- *specimen tested with rectangular pipes at the back of the top and bottom courses of the specimen (pinned–pinned);* **SB3**- *post-tensioned rebar on both side like column;* **SB4**- *returning wall on both side rest against strong resistance wall;* **LT1**- *four-point loading with two loading points each @ approx. span/3;* **LT2**- *four-point loading with two main loading points each @ approx. span/3 and multiple loading points @ span/6*

REF	Type	Brick (N/mm^2)	Mortar (N/mm^2)	Geometry (h × l × t in mm)	Slenderness ratio (h/l)	Qty	Standard	Support-Bottom	Support-Top	Support-Back	Loading Type	Loading Rate	Instrument	Measured	Plot	Estimated-results	Failure Mode
[60]	OOP-HOR	50.9	21.59	1460 × 500 × 230	2.9	3	N/A	free	free	SB1	four-point loading	gradually	load cell and LVDTs	load and displacement	load – displacement	first crack, deflection stiffness	cracks at the joint near mid-height to split specimen into two
[27]	OOP-HOR	23.3	6.73	300 ×150 × 50	2	3	ASTM E518 −15	free	free	SB1	four-point loading	gradually	load cell and LVDTs	load and displacement	n/a	peak load, displacement and flexural strength	splitting of joints or contact areas that later pass through brick/unit
[61]	OOP-HOR	21.2	6.54	1340 × 440 × 102.5	3	3	n/a	free	free	SB1	three-point loading	0.017 mm/s	load cell and LVDTs	load and displacement	load – displacement	maximum load and mid-displacement	cracks at the joint near the load point to split the specimen into two
[62]	OOP-HOR	24.42	5.99	4000 × 500 × 500	8	4	n/a	free	free	SB2	four-point loading	incremental	load weight and sensor	load and displacement	load – displacement	deflection and load	cracks at the joint near the load point to split the specimen into two
[63]	OOP	19.01	3.8	2660 × 2430 × 240 1250 U shape	1.1	2	n/a	free	free	SB4	two-point loading at the top and bottom	40–60 N/s	load cell and LVDTs	load and displacement	load – displacement	flexural strength and maximum displacement	three hinges on the face-loaded wall at the base, top and near the point of load application.
[64]	OOP	82.1	14.29	1350 × 2250 × 300 U shape	1.7	3	n/a	BOT2	TOP1	SB4	UDL using airbag against the wall	gradually	load cell and LVDTs	load and displacement	load – displacement	stiffness	cracks extending from the top to the bottom of the front elevation.

OOP: Out-of-plane loading at middle of the wall in vertical position; OOP-HOR: Out-of-plane loading at middle of the wall in horizontal position

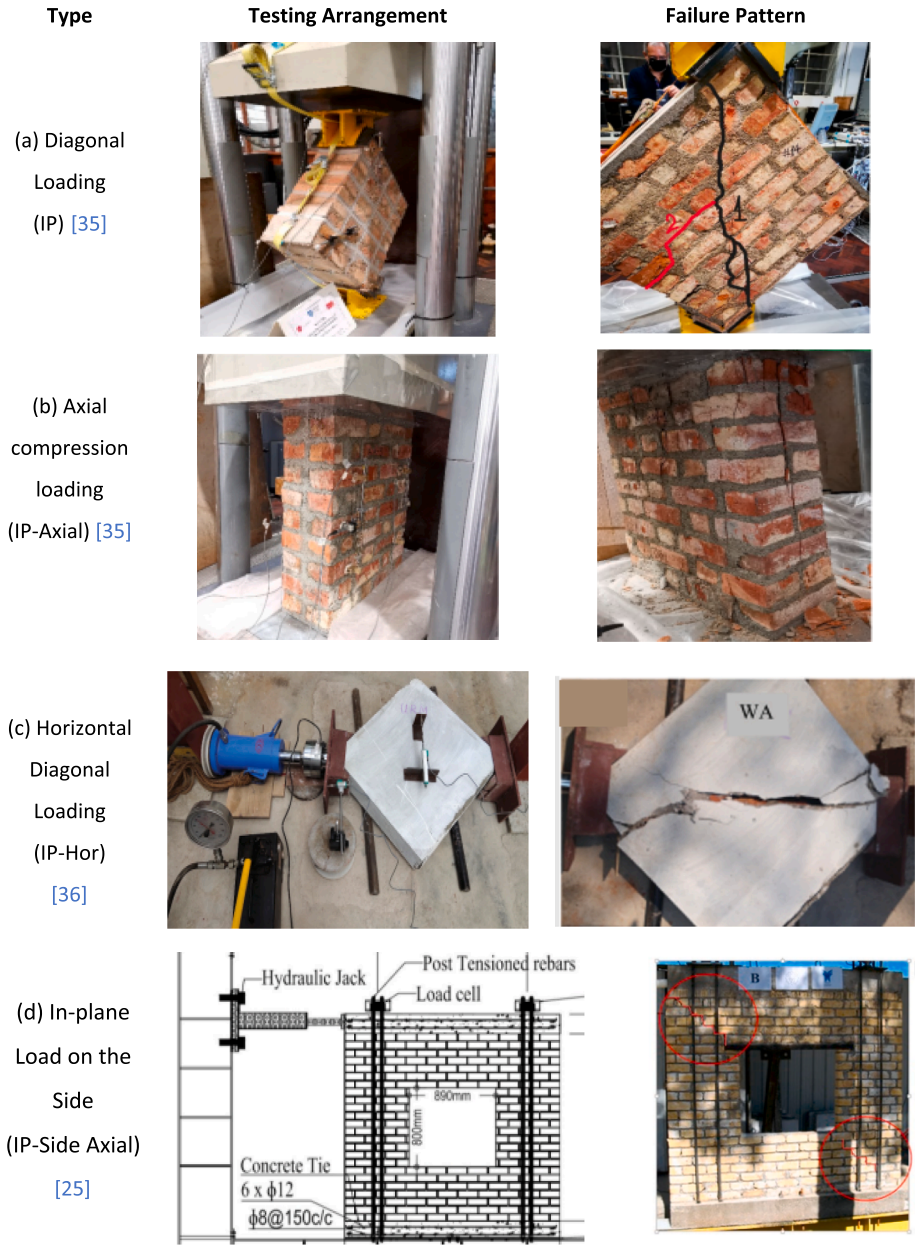

Fig. 4. In-plane testing arrangement and failure pattern.

studies with others showing variations across different testing arrangements. Specifically, the study highlighted that a material combination with masonry units having higher strength than the mortar joints is often common in experimental studies of masonry behaviour. This is because such combination replicates the pattern found in masonry building which is the stronger unit-weaker joint. The review shows that this combination often results in the failure of joint rather than unit. This means that the strength of the mortar joint and bonding pattern is very influential in the structural performance of masonry structures and as such should be closely considered when evaluating masonry wall performance.

In general, it can be concluded that most experimental testing of masonry walls focused on walls without openings or one-centred openings. This narrow focus leads to an incomplete understanding and to inaccurate predictions of the masonry behaviour in practical applications because it may neglect the common real-world scenario of walls with openings. Moreover, the general dimensions of the tested walls are often small and slender, typically consisting of a single wythe of bricks. Although it is noted that strength tends to rise with wall thickness, there are still few experimental campaigns conducted on thick URM walls. This again shows the variation between the real-world application of masonry walls and the scenario in which they are tested/assessed in the laboratory.

From the conducted review, it is possible to acknowledge the lack of consistency in the definition of the specimens' geometry,

boundary conditions, loading rates, and specific experimental setup across several studies. The lack of a specific guideline governing the experimental procedures for assessing the IP and OOP behaviour of masonry walls may contribute to the latter. Several standardised protocols led to the development of various test setups, each with unique characteristics, which may contribute to the complexity of the interpretation of results. Although the direct comparison between experimental data can be complex due to the different geometries adopted, such variability can in some extent enrich the literature available for numerical validation studies. The choice over the adopted geometry and size may often be conditioned by limitations on the testing facilities and available funding. Although the geometry can govern explicitly the failure mode obtained, the advantages in the use of larger setups can be arguable, as for instance to characterise failure modes that are mainly governed by one-way bending (horizontal or vertical) [21,34,41,66].

Nonetheless, the use of consistent features for the testing can provide the possibility of studying the role of uncertainty in the mechanical response of masonry walls. Data on the material, spatial and quality-labour related uncertainties are still scarce in the literature [67–69], and the use of consistent testing schemes may, ultimately, lead to refine the design of probabilistic-based guidelines and standards for masonry structures [67,69]. On the other hand, as it is demonstrated, the effect of the irregular disposition of openings on the mechanical response of masonry walls needs to be better addressed, as somehow pointed out in a recent study with

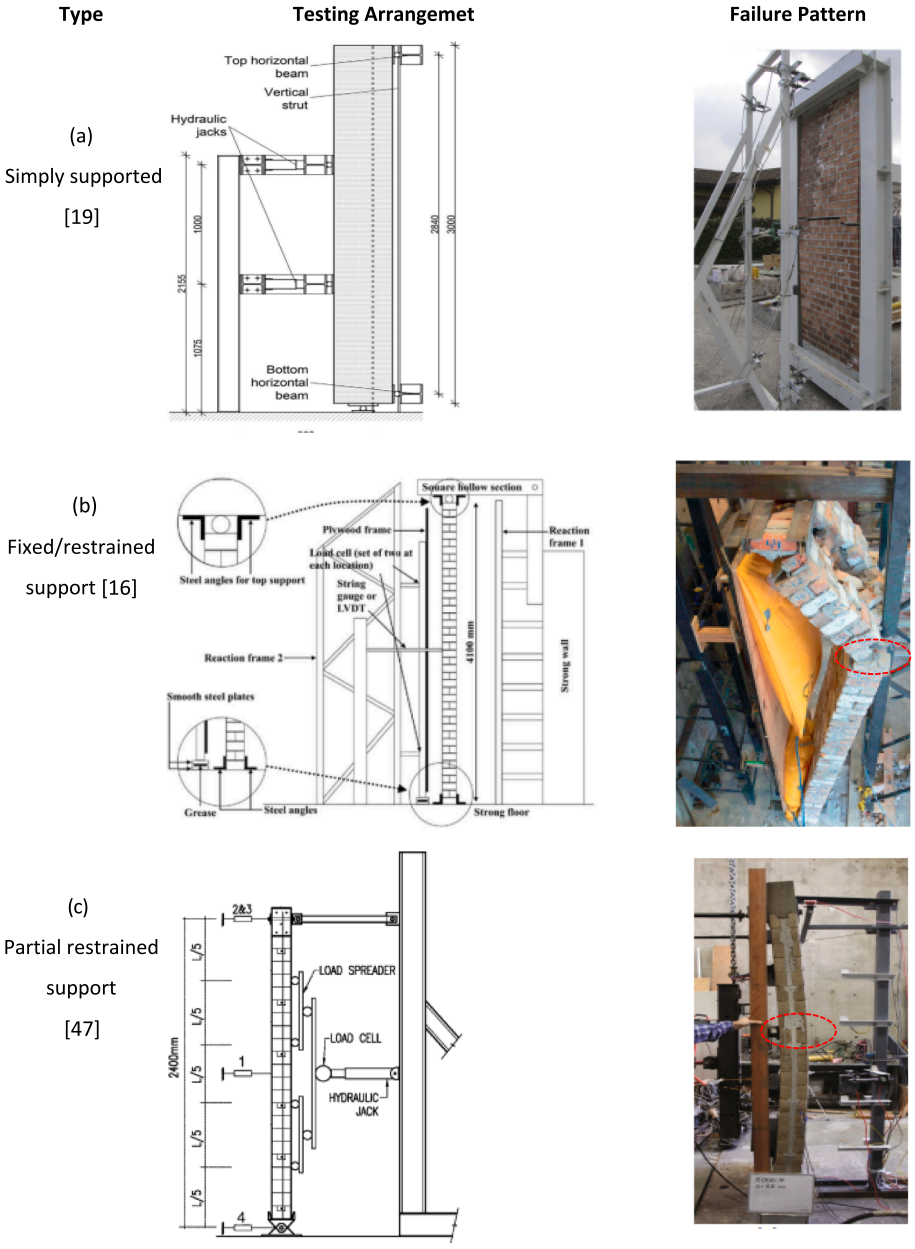

Fig. 5. Out-of-testing arrangement.

different numerical approaches [70,71] as well as the interaction with transversal walls and slabs/connections [72].

The study thus recommends further experimental studies on the effect of openings on walls and the interaction between masonry walls and the slabs/connections with other walls/ring beams to enrich masonry behaviour understanding through both experimental and numerical approaches.

CRediT authorship contribution statement

Jamiu A. Dauda: Writing – original draft, Methodology, Conceptualization. **Ornella Iuorio:** Supervision, Conceptualization. **Imrose B. Muhit:** Writing – review & editing, Validation. **Luis C.M. da Silva:** Writing – review & editing.

Declaration of competing interest

The authors declare that they have no known competing financial interests or personal relationships that could have appeared to influence the work reported in this paper.

Data availability

Data will be made available on request.

References

[1] G. Vasconcelos, P.B. Lourenço, Experimental characterization of stone masonry in shear and compression, Constr. Build. Mater. 23 (2009) 3337–3345, https://doi.org/10.1016/j.conbuildmat.2009.06.045.
[2] O. Iuorio, J.A. Dauda, P.B. Lourenço, Experimental evaluation of out-of-plane strength of masonry walls retrofitted with oriented strand board, Constr. Build. Mater. 269 (2021) 121358, https://doi.org/10.1016/j.conbuildmat.2020.121358.
[3] G.H. Nalon, J.C.L. Ribeiro, L.G. Pedroti, R.M. da Silva, E.N.D. de Araújo, R.F. Santos, G.E.S. de Lima, Review of recent progress on the compressive behavior of masonry prisms, Constr. Build. Mater. 320 (2022) 126181, https://doi.org/10.1016/j.conbuildmat.2021.126181.
[4] British Standards Institution, BS EN 1996-1-1:2005: Eurocode 6 -Design of Masonry Structures - Part 1-1: General Rules for Reinforced and Unreinforced Masonry Structures., 1 (1996).
[5] J.A. Dauda, L.C. Silva, P.B. Lourenço, O. Iuorio, Engineering structures out-of-plane loaded masonry walls retrofitted with oriented strand boards: numerical analysis and influencing parameters, Eng. Struct. 243 (2021) 112683, https://doi.org/10.1016/j.engstruct.2021.112683.
[6] A. Rezaie, M. Godio, K. Beyer, Experimental investigation of strength, stiffness and drift capacity of rubble stone masonry walls, Constr. Build. Mater. 251 (2020) 118972, https://doi.org/10.1016/j.conbuildmat.2020.118972.
[7] S. Nazir, Studies on the Failure of Unreinforced Masonry Shear Walls. A Thesis Submitted in Partial Fulfilment of the Requirements for the Degree of Doctor of Philosophy (PhD), Queensland University of Technology, Australia, 2015.
[8] J. Segura, E. Bernat, V. Mendizábal, L. Pelà, P. Roca, L. Gil, Experimental comparison of two testing setups for characterizing the shear mechanical properties of masonry, J. Build. Eng. 44 (2021) 103277, https://doi.org/10.1016/j.jobe.2021.103277.
[9] J.A. Dauda, Numerical and Experimental Investigation of Unreinforced Masonry Wall Retrofitted with Timber Panels, University of Leeds, UK, 2020.
[10] P.G. Asteris, V. Plevris, eds., Handbook of Research on Seismic Assessment and Rehabilitation of Historic Structures, IGI Global, 2015. DOI: 10.4018/978-1-4666-8286-3.
[11] J.A. Dauda, O. Iuorio, P.B. Lourenço, Numerical analysis and experimental characterisation of brick masonry, Int. J. Mason. Res. Innov. (2020), https://doi.org/10.1504/IJMRI.2020.107994.
[12] G. Vasconcelos, Experimental investigations on the mechanics of stone masonry: Characterization of granites and behaviour of ancient masonry shear walls, University of Minho, Guimarães, Portugal, 2005.
[13] N. Ismail, N. Khattak, Observed failure modes of unreinforced masonry buildings during the 2015 Hindu Kush earthquake, Earthq. Eng. Eng. Vib. 18 (2019) 301–314. DOI: 10.1007/s11803-019-0505-x.
[14] A.A. Costa, A. Arêde, A. Costa, C.S. Oliveira, Out-of-plane behaviour of existing stone masonry buildings: experimental evaluation, Bull. Earthq. Eng. 10 (2012) 93–111, https://doi.org/10.1007/s10518-011-9332-9.
[15] Y. Pan, X. Wang, R. Guo, S. Yuan, Seismic damage assessment of Nepalese cultural heritage building and seismic retrofit strategies: 25 April 2015 Gorkha (Nepal) earthquake, Eng. Fail. Anal. 87 (2018) 80–95. DOI: 10.1016/j.engfailanal.2018.02.007.
[16] T. T. Bui, A. Limam, E. Ferrier, M. Brun, D. Bertrand, Masonry walls submitted to out-of-plane loading: Experimental and numerical study, Proc. 8th Int. Mason. Conf. (2010) 1153-1162.
[17] Y. Lin, D. Lawley, L. Wotherspoon, J.M. Ingham, Out-of-plane testing of unreinforced masonry walls strengthened using ECC shotcrete, Structures. 7 (2016) 33–42, https://doi.org/10.1016/j.istruc.2016.04.005.
[18] E. Minaie, Behavior and Vulnerability of Reinforced Masonry Shear Walls, Drexel University, 2009.
[19] J. Brunner, Shear strength of reinforced masonry walls, University of Colorado (1994).
[20] N. Gattesco, I. Boem, Experimental and analytical study to evaluate the effectiveness of an in-plane reinforcement for masonry walls using GFRP meshes, Constr. Build. Mater. 88 (2015) 94–104, https://doi.org/10.1016/j.conbuildmat.2015.04.014.
[21] P.B. Lourenço, N. Mendes, A.A. Costa, A. Campos-Costa, Methods and challenges on the out-of-plane assessment of existing masonry buildings, Int. J. Archit. Herit. (2016) 1, https://doi.org/10.1080/15583058.2017.1237114.
[22] T. David, Gough; Sandy, Oliver; James, An introduction to systematic reviews, SAGE Publications, Los Angeles, 2017.
[23] A. Saad, S.O. Ajayi, H.A. Alaka, Trends in BIM-based plugins development for construction activities: a trends in BIM-based plugins development for construction activities: a systematic review, Int. J. Constr. Manage. (2022) 1–13, https://doi.org/10.1080/15623599.2022.2093815.
[24] R. Dekkers, L. Carey, P. Langhorne, Setting Inclusion and Exclusion Criteria, in: Mak. Lit. Rev. Work A Multidiscip. Guid. to Syst. Approaches, Springer International Publishing, Cham, 2022: pp. 201–233. DOI: 10.1007/978-3-030-90025-0_6.
[25] A.R. Kamrava, M.A. Najafgholipour, F. Fathi, S.M. Dehghan, An experimental study on the in-plane behavior of unreinforced masonry walls with an opening strengthened using steel fiber reinforced concrete overlays, J. Build. Eng. 36 (2021) 102084, https://doi.org/10.1016/j.jobe.2020.102084.
[26] S. Babaeidarabad, F. De Caso, A. Nanni, URM walls strengthened with fabric-reinforced cementitious matrix composite subjected to diagonal compression, J. Compos. Constr. 18 (2014), https://doi.org/10.1061/(asce)cc.1943-5614.0000441.
[27] V. Baneshi, S.M. Dehghan, R. Hassanli, An experimental study on the behavior of interlocking masonry blocks manufactured using 3D printed mold, Adv. Struct. Eng. 26 (2023) 360–380, https://doi.org/10.1177/13694332221126595.
[28] J. Segura, L. Pelà, S. Saloustros, P. Roca, Experimental and numerical insights on the diagonal compression test for the shear characterisation of masonry, Constr. Build. Mater. 287 (2021) 122964, https://doi.org/10.1016/j.conbuildmat.2021.122964.

[29] I. Giongo, E. Rizzi, D. Riccadonna, M. Piazza, On-site testing of masonry shear walls strengthened with timber panels, Proc. Inst. Civ. Eng. Struct. Build. 174 (2021) 389–402, https://doi.org/10.1680/jstbu.19.00179.
[30] J. Donnini, G. Maracchini, S. Lenci, V. Corinaldesi, E. Quagliarini, TRM reinforced tuff and fired clay brick masonry: experimental and analytical investigation on their in-plane and out-of-plane behavior, Constr. Build. Mater. 272 (2021) 121643, https://doi.org/10.1016/j.conbuildmat.2020.121643.
[31] E. Mustafaraj, Y. Yardim, M. Corradi, A. Borri, Polypropylene as a retrofitting material for shear walls, Materials (Basel) 13 (2020), https://doi.org/10.3390/ma13112503.
[32] E. Mustafaraj, Y. Yardim, In-plane shear strengthening of unreinforced masonry walls using GFRP jacketing.pdf, Period. Polytech. Civ. Eng. 62 (2018) 330–336.
[33] G. Marcari, M. Basili, F. Vestroni, Experimental investigation of tuff masonry panels reinforced with surface bonded basalt textile-reinforced mortar, Compos. Part B Eng. 108 (2017) 131–142, https://doi.org/10.1016/j.compositesb.2016.09.094.
[34] G. Castori, M. Corradi, E. Sperazini, Full size testing and detailed micro-modeling of the in-plane behavior of FRCM–reinforced masonry, Constr. Build. Mater. 299 (2021) 124276, https://doi.org/10.1016/j.conbuildmat.2021.124276.
[35] A. Demaj, A.S. Gago, A.I. Marques, J.G. Ferreira, In-plane seismic behavior of brick masonry walls reinforced with twisted steel bars and conventional steel bars, Buildings. 12 (2022) 1–24, https://doi.org/10.3390/buildings12040421.
[36] T. Warjri, D.F. Marbaniang, C. Marthong, In-plane behaviour of masonry walls embedding with steel welded wire mesh overlay with mortar, J. Struct. Integr. Maint. 7 (2022) 177–187, https://doi.org/10.1080/24705314.2022.2048241.
[37] T. Zahra, J. Thamboo, M. Asad, M. Song, Experimental investigation on the effectiveness of lateral restrainers to the vertical steel in reinforced masonry walls under axial compression, Constr. Build. Mater. 297 (2021) 123790, https://doi.org/10.1016/j.conbuildmat.2021.123790.
[38] T. Zahra, J. Dorji, J. Thamboo, N. Cameron, M. Asad, W. Kasinski, A. Nardone, Behaviour of reinforced mortarless concrete masonry panels under axial compression: An experimental and analytical study, Constr. Build. Mater. 377 (2023) 131097, https://doi.org/10.1016/j.conbuildmat.2023.131097.
[39] N. Grillanda, A. Chiozzi, G. Milani, A. Tralli, Tilting plane tests for the ultimate shear capacity evaluation of perforated dry joint masonry panels. Part I: Experimental tests, Eng. Struct. 238 (2021) 112124, https://doi.org/10.1016/j.engstruct.2021.112124.
[40] N. Ismail, J.M. Ingham, In-plane and out-of-plane testing of unreinforced masonry walls strengthened using polymer textile reinforced mortar, Eng. Struct. 118 (2016) 167–177, https://doi.org/10.1016/j.engstruct.2016.03.041.
[41] I.B. Muhit, M.J. Masia, M.G. Stewart, Monte-Carlo laboratory testing of unreinforced masonry veneer wall system under out-of-plane loading, Constr. Build. Mater. 321 (2022) 126334, https://doi.org/10.1016/j.conbuildmat.2022.126334.
[42] S. Babaeidarabad, F. De Caso, A. Nanni, Out-of-plane behavior of URM walls strengthened with fabric-reinforced cementitious matrix composite, J. Compos. Constr. 18 (2014), https://doi.org/10.1061/(asce)cc.1943-5614.0000457.
[43] M. Kałuża, J. Hulimka, J. Kubica, Experimental studies of external panels as a method of structural failure prevention, Eng. Fail. Anal. 146 (2023), https://doi.org/10.1016/j.engfailanal.2023.107114.
[44] B.R. Robazza, S. Brzev, T.Y. Yang, K.J. Elwood, D.L. Anderson, B. McEwen, Out-of-Plane behavior of slender reinforced masonry shear walls under in-plane loading: experimental investigation, J. Struct. Eng. 144 (2018) 1–16, https://doi.org/10.1061/(asce)st.1943-541x.0001968.
[45] M. Martínez, S. Atamturktur, Experimental and numerical evaluation of reinforced dry-stacked concrete masonry walls, J. Build. Eng. 22 (2019) 181–191, https://doi.org/10.1016/j.jobe.2018.12.007.
[46] T. Zahra, J. Thamboo, J. Dorji, M. Asad, W. Kasinski, A. Nardone, Out-of-plane flexural behaviour of reinforced mortarless concrete block masonry: an experimental study, Constr. Build. Mater. 384 (2023) 131448, https://doi.org/10.1016/j.conbuildmat.2023.131448.
[47] P.T. Laursen, N.A. Herskedal, D.C. Jansen, B. Qu, Out-of-plane structural response of interlocking compressed earth block walls, Mater. Struct. Constr. 48 (2015) 321–336, https://doi.org/10.1617/s11527-013-0186-2.
[48] P. Kasinikota, D.D. Tripura, Flexural behavior of hollow interlocking compressed stabilized earth-block masonry walls under out-of-plane loading, J. Build. Eng. 57 (2022) 104895, https://doi.org/10.1016/j.jobe.2022.104895.
[49] T.M. Ferreira, A.A. Costa, A. Arêde, A. Gomes, A. Costa, Experimental characterization of the out-of-plane performance of regular stone masonry walls, including test setups and axial load influence, Bull. Earthq. Eng. 13 (2015) 2667–2692, https://doi.org/10.1007/s10518-015-9742-1.
[50] P.K.V.R. Padalu, Y. Singh, S. Das, Out-of-plane flexural strengthening of URM wallettes using basalt fibre reinforced polymer composite, Constr. Build. Mater. 216 (2019) 272–295, https://doi.org/10.1016/j.conbuildmat.2019.04.268.
[51] H. Derakhshan, D. Dizhur, M.C. Griffith, J.M. Ingham, In situ out-of-plane testing of as-built and retrofitted unreinforced masonry walls, J. Struct. Enginee. 01 (2014) 1–23.
[52] N. Gattesco, I. Boem, Out-of-plane behavior of reinforced masonry walls: Experimental and numerical study, Compos. Part B Eng. 128 (2017) 39–52, https://doi.org/10.1016/j.compositesb.2017.07.006.
[53] J.A. Dauda, P. Lourenço, O. Iuorio, Out-of-plane testing of masonry walls retrofitted with oriented strand board (OSB) timber panels, Proc. Inst. Civ. Eng. - Struct. Build. (2020) 1–33, https://doi.org/10.1680/jstbu.19.00095.
[54] K.Q. Walsh, D.Y. Dizhur, J. Shafaei, H. Derakhshan, J.M. Ingham, In situ out-of-plane testing of unreinforced masonry cavity walls in as-built and improved conditions, Structures. 3 (2015) 187–199, https://doi.org/10.1016/j.istruc.2015.04.005.
[55] Y. Lin, D. Lawley, L. Wotherspoon, J.M. Ingham, 24-2016-Out-of-plane Testing of Unreinforced Masonry Walls Strengthened Using ECC Shotcrete.pdf, Structures. 7 (2016).
[56] D. Dizhur, M. Griffith, J. Ingham, Out-of-plane strengthening of unreinforced masonry walls using near surface mounted fibre reinforced polymer strips, Eng. Struct. 59 (2014) 330–343, https://doi.org/10.1016/j.engstruct.2013.10.026.
[57] H. Derakhshan, M.C. Griffith, J.M. Ingham, Airbag testing of multi-leaf unreinforced masonry walls subjected to one-way bending, Eng. Struct. 57 (2013) 512–522, https://doi.org/10.1016/j.engstruct.2013.10.006.
[58] S. Banerjee, S. Nayak, S. Das, Enhancing the flexural behaviour of masonry wallet using PP band and steel wire mesh, Constr. Build. Mater. 194 (2019) 179–191, https://doi.org/10.1016/j.conbuildmat.2018.11.001.
[59] M. Corradi, A. Borri, G. Castori, R. Sisti, The Reticulatus method for shear strengthening of fair-faced masonry, Bull. Earthq. Eng. 14 (2016) 3547–3571, https://doi.org/10.1007/s10518-016-0006-5.
[60] E. Ferretti, G. Pascale, Combined strengthening techniques to improve the out-of-plane performance of masonry walls, Materials (basel). 12 (2019), https://doi.org/10.3390/ma12071171.
[61] F.A. Kariou, S.P. Triantafyllou, D.A. Bournas, L.N. Koutas, Out-of-plane response of masonry walls strengthened using textile-mortar system, Constr. Build. Mater. 165 (2018) 769–781, https://doi.org/10.1016/j.conbuildmat.2018.01.026.
[62] R. Sisti, M. Corradi, A. Borri, An experimental study on the influence of composite materials used to reinforce masonry ring beams, Constr. Build. Mater. 122 (2016) 231–241, https://doi.org/10.1016/j.conbuildmat.2016.06.120.
[63] M. Corradi, E. Speranzini, G. Bisciotti, Out-of-plane reinforcement of masonry walls using joint-embedded steel cables, Bull. Earthq. Eng. 18 (2020) 4755–4782, https://doi.org/10.1007/s10518-020-00875-3.
[64] A. Murano, J. Ortega, G. Vasconcelos, H. Rodrigues, Influence of traditional earthquake-resistant techniques on the out-of-plane behaviour of stone masonry walls: experimental and numerical assessment, Eng. Struct. 201 (2019) 109815, https://doi.org/10.1016/j.engstruct.2019.109815.
[65] UMINHO (2006). Review on the Experimental In-Plane and Out-of-Plane Testing: Developing Innovative Systems for Reinforced Masonry Walls. [online] Italy: Università di Padova (Italy). Available at: http://diswall.dic.unipd.it/Results/D5.1_FINAL.pdf [Accessed 14 Mar. 2024].
[66] F. Graziotti, U. Tomassetti, S. Sharma, L. Grottoli, G. Magenes, Experimental response of URM single leaf and cavity walls in out-of-plane two-way bending generated by seismic excitation, Constr. Build. Mater. 195 (2019) 650–670, https://doi.org/10.1016/j.conbuildmat.2018.10.076.
[67] J. Haddad, S. Cattari, S. Lagomarsino, Use of the model parameter sensitivity analysis for the probabilistic-based seismic assessment of existing buildings, Bull Earthquake Eng 17 (2019) 1983–2009, https://doi.org/10.1007/s10518-018-0520-8.
[68] M. Tondelli, M. Rota, A. Penna, G. Magenes, Evaluation of uncertainties in the seismic assessment of existing masonry buildings, J. Earthq. Engi. 16 (2012) 36–64, https://doi.org/10.1080/13632469.2012.670578.

[69] I.B. Muhit, M.J. Masia, M.G. Stewart, Failure analysis and structural reliability of unreinforced masonry veneer walls: Influence of wall tie corrosion, Eng. Fail. Anal. 151 (2023) 107354, https://doi.org/10.1016/j.engfailanal.2023.107354.
[70] F. Parisse, V. Buonocunto, C. Cantagallo, A. Di Primio, E. Di Domenico, N. Lo Presti, ... S. Cattari, Investigating the seismic response of URM walls with irregular opening layout through different modeling approaches. In COMPDYN Proceedings (2023) 1906-1920, National Technical University of Athens.
[71] C. Morandini, D. Malomo, A. Penna, Equivalent frame discretisation for URM façades with irregular opening layouts, Bull. Earthq. Eng. 20 (2022) 2589–2618, https://doi.org/10.1007/s10518-022-01315-0.
[72] A. Barontini, J. Scacco, L.C. da Silva, G. Vasconcelos, P.B. Lourenço, G. Milani, Experimental quasi-static out-of-plane test of a U-shaped brick masonry wall, Eng. Struct. 287 (2023) 116195, https://doi.org/10.1016/j.engstruct.2023.116195.